Mineralogical Magazine, February 2002, Vol. 66(1), pp. 137–150

Manganvesuvianite and tweddillite, two new Mn^{3+}-silicate minerals from the Kalahari manganese fields, South Africa

T. ARMBRUSTER[1,*], E. GNOS[2], R. DIXON[3], J. GUTZMER[4], C. HEJNY[5], N. DÖBELIN[5] AND O. MEDENBACH[6]

[1] Laboratorium für chemische und mineralogische Kristallographie, Universität Bern, Freiestrasse 3, CH-3012 Bern, Switzerland
[2] Mineralogisch-Petrographisches Institut, Baltzerstrasse 1, CH-3012 Bern, Switzerland
[3] Private Bag X620, Pretoria 0001, Republic of South Africa
[4] Department of Geology, Rand Afrikaans University, P.O. Box 524, Auckland Park 2006, Republic of South Africa
[5] Laboratorium für chemische und mineralogische Kristallographie, Universität Bern, Freiestrasse 3, CH-3012 Bern, Switzerland
[6] Institut für Geologie, Mineralogie und Geophysik, Ruhr-Universität, D-44780 Bochum, Germany

ABSTRACT

The new minerals manganvesuviante and tweddillite, both formed by hydrothermal alteration of primary manganese ores, are described from the Kalahari manganese fields (Republic of South Africa). In addition, single-crystal X-ray structure refinements of both new minerals are presented.

Manganvesuvianite is a tetragonal vesuvianite mineral with the simplified formula $Ca_{19}Mn^{3+}(Al,Mn^{3+},Fe^{3+})_{10}(Mg,Mn^{2+})_2Si_{18}O_{69}(OH)_9$, characterized by Mn^{3+} occupying the five-coordinated position (square pyramid). The crystals have simple prismatic forms: [100], [110] terminated by [101] and exhibit deep maroon red colour. With polarized light the crystals are strongly pleochroic, yellowish parallel to E and dark red to lilac parallel to O.

Tweddillite is an epidote-group mineral (space group space group $P2_1/m$, a = 8.932(5), b = 5.698(4), c = 10.310(5) Å, β = 114.56(4), V = 477.3(8) Å^3) with the simplified formula $CaSr(Mn^{3+},Fe^{3+})_2Al\{Si_3O_{12}\}(OH)$, closely related to strontiopiemontite. The difference between strontiopiemontite and tweddillite is the concentration of octahedral Mn^{3+}. Strontiopiemontite has Mn^{3+} mainly on the $M3$ site whereas tweddillite has Mn^{3+} with minor Fe^{3+} on $M3$ and $M1$. Tweddillite forms aggregates of very thin dark red [001] blades characterized by striking pleochroism. The crystals appear dark red parallel to b and orange-yellow parallel to a. Perpendicular to (001) the blades appear magenta to red.

KEYWORDS: manganvesuvianite, tweddillite, Kalahari, manganese fields, South Africa, epidote group, vesuvianite.

Introduction

A variety of rather rare manganese minerals formed in the Kalahari manganese fields by hydrothermal alteration (250–400°C) of the primary sedimentary and low-grade metamorphic manganese ores. Such minerals crystallized along fault planes and lenticular bodies within the manganese ore beds or filling veins and vugs (Cairncross *et al.*, 1997).

Recently, the IMA Commission on New Minerals and Mineral Names (CNMMN) approved two new mineral species from this locality which are characterized, including their crystal structures. Both new species manganvesuvianite (CNMMN-2000-40) and tweddillite (CNMMN-2001-14) belong to well established mineral groups, the vesuvianite and epidote minerals, respectively.

Manganvesuvianite

General aspects of vesuvianite crystal chemistry

A simplified formula of tetragonal vesuvianite (a ≈ 15.5, c ≈ 11.8 Å, Z = 2), taking into account

* E-mail: thomas.armbruster@krist.unibe.ch
DOI: 10.1180/002646102661001 8

the various cation coordinations and its domain structure, may be written as $X_{18}X'Y'Y2_4\ Y3_8\ Z_{18}O_{69}(OH,F)_9$ where X and X' are seven to nine-coordinated, $Y2$ and $Y3$ have octahedral coordination, Y' has square pyramidal coordination, and Z represents tetrahedral coordination. X and X' are commonly occupied by Ca. Y and Y' host elements with an average valence of 2.85 (e.g. 11 Al and 2 Mg) and Z is mainly occupied by Si. X' and Y' occupy strings along the 4-fold axes. In space group $P4/nnc$, these strings have the sequence $Y'X'X'Y'$ but due to short $X'X'$ and $Y'X'$ distances, occupied sites always alternate with vacancies (□). Thus a string along a 4-fold axis has locally either a $Y'\square X'\square$ or a $\square X'\square Y'$ arrangement. If we assume for electrostatic reasons that two adjacent vacancies do not occur, each string itself is fully ordered (short range ordering). However, adjacent strings are either long-range disordered (space group $P4/nnc$) or they follow some specific ordering patterns leading to decreased symmetry (Giuseppetti and Mazzi, 1983; Fitzgerald *et al.*, 1986; Allen and Burnham, 1992; Ohkawa *et al.*, 1994; Pavese *et al.*, 1998; Armbruster and Gnos, 2000*a,b,c*).

In addition to these 'common vesuvianites' there are also excess *Y*-group vesuvianites (Groat *et al.*, 1994*a,b*) with additional sites occupied that are vacant in ordinary vesuvianites. These additional sites may also be occupied by boron leading to wiluite (Groat *et al.*, 1998) of simplified composition $Ca_{19}(Al,Mg,Fe,Ti)_{13}(B,Al,\square)_5Si_{18}O_{68}(O,OH)_{10}$.

The IMA CNMMN (Nickel and Grice, 1998) has defined the general guideline for compositional criteria that at least one structural site in the potential new mineral should be predominantly occupied by a different chemical component than that which occurs in the equivalent site in an existing mineral species. This rule expands vesuvianite to a mineral group with various mineral species distinguished by different cations occupying the square pyramidal Y' site. Ohkawa *et al.* (1992) suggest that Mn^{2+}, Fe^{2+}, Cu^{2+}, Fe^{3+} and Mg^{2+} may occupy the five-coordinated Y' site. However, interatomic distances obtained from diffraction experiments of disordered $P4/nnc$ vesuvianites are not reliable for assignments of cation radii to the Y' site because in $P4/nnc$ symmetry this site is only 50% occupied with the remaining 50% being vacancies. In other words, the valence of Mn and Fe cannot simply be derived from interatomic distances. High-resolution solid-state ^{27}Al NMR spectroscopy (Phillips *et al.*, 1987; Olejniczak and Zabinski, 1996) indicated that in Mg-rich (Fe-poor) vesuvianites also, Al may dominate the five-coordinated site. In a combined X-ray and neutron diffraction study Pavese *et al.* (1998) have shown that in a $P4/n$ vesuvianite from Val d'Ala (Italy) the square pyramidal Y' site is occupied by Fe^{3+}. The examples above demonstrate that the vesuvianite group is much more complex than hitherto assumed, requiring definition of new mineral species.

Definition

Manganvesuvianite is a vesuvianite group mineral where the five-coordinated (Y') position (square pyramid) is occupied by Mn^{3+}. The simplified formula is $Ca_{19}Mn^{3+}(Al,Mn^{3+},Fe^{3+})_{10}(Mg,Mn^{2+})_2Si_{18}O_{69}(OH)_9$.

Identification criteria

(1) Manganvesuvianite is macroscopically deep red and strongly pleochroic E: colourless–yellowish, O: dark red or lilac. More detailed optical absorption spectra of five-coordinated Mn^{3+} in vesuvianite are discussed by Hålenius and Annersten (1994) and Platonov *et al.* (1995).

(2) If the chemical formula of a boron-poor vesuvianite is either normalized to 50 cations or (Ca + Sr + Ba + Na + K) = 19, there are 13 *Y* type cations (Al, Fe^{3+}, Mn^{3+}, Mg, Fe^{2+}, Mn^{2+}, Cu^{2+}, Ti^{4+}). For stoichiometry reasons the average charge of the *Y* cations must be 2.85^+. If Ti^{4+} can be ignored (which is the case for the Mn-rich samples described here) two *Y* cations are divalent and eleven *Y* cations are trivalent. The divalent *Y* cations are Mg, Cu^{2+} and Mn^{2+}. If the analysis reveals, after correction for Mn^{2+} (2 − (Mg + Cu) p.f.u. = Mn^{2+} pfu), more than 1 Mn^{3+} p.f.u. and in addition $Mn^{3+} > Fe^{3+}$, the mineral is manganvesuvianite.

(3) Crystal structure analysis of manganvesuvianite indicates that Mn^{3+} occupies the five-coordinated square pyramidal Y' position leading to Jahn-Teller distortion where the four-fold axis of the square pyramid is elongated.

Occurrence

Manganvesuvianite (Wessels mine and N'Chwaning II mine) occurs as long prismatic (up to 1.5 cm) crystals filling veins and vugs. Larger crystals are nearly black and opaque with

TABLE 1. Electron microprobe analyses of manganvesuvianites from the N'Chwaning II mine.

	NC14-38[1]	NCII-1[2]	St. dev.	NCII-2[3]	St. dev.
SiO_2	34.13	36.69	0.16	36.15	0.43
TiO_2	0.00	0.00	0.00	0.00	0.00
Al_2O_3	10.63	16.19	0.32	14.73	0.63
Fe_2O_3	0.00	1.83	0.16	1.12	0.60
Mn_2O_3	15.96	3.78	0.19	6.79	1.01
MgO	0.09	2.47	0.24	2.35	0.30
CaO	34.33	36.07	0.16	35.73	0.22
CuO	0.41	0.06	0.05	0.02	0.02
SrO	0.05	0.12	0.06	0.11	0.06
BaO	0.00	0.00	0.00	0.00	0.00
Na_2O	0.00	0.05	0.03	0.03	0.02
K_2O	0.01	0.00	0.01	0.00	0.00
F	0.12	0.05	0.04	0.12	0.06
Cl	0.00	0.01	0.01	0.01	0.01
H_2O (calc.)	2.52	2.74	0.02	2.67	0.04
−(F+Cl)	−0.06	−0.03		−0.07	
Sum	98.19	100.03		99.76	
Formulae normalized to (Ca + Sr + Ba + Na + K) = 19					
Si	17.611	17.962		17.885	
Ti	0.000	0.000		0.000	
Al	6.467	9.341		8.589	
Mn^{3+}	4.498	1.226		2.300	
Mn^{2+}	1.770	0.175		0.260	
Fe^{3+}	0.000	0.675		0.418	
Fe^{2+}	0.000	0.000		0.000	
Mg	0.072	1.803		1.733	
Ca	18.972	18.918		18.940	
Cu	0.158	0.022		0.007	
Sr	0.014	0.034		0.032	
Ba	0.000	0.000		0.000	
Na	0.000	0.047		0.029	
K	0.009	0.000		0.000	
F	0.191	0.077		0.188	
Cl	0.000	0.008		0.008	
H (calc.)		8.914		8.804	
Sum *Y*[4]	12.965	13.242		13.308	

[1] Armbruster and Gnos (2000*b*)
[2] Sample for refractive index measurement (average of 15 point analyses)
[3] Sample for crystal structure analysis (average of 19 point analyses)
[4] Excess of *Y* cations (Al + Fe +Mg + Mn + Cu + Ti) > 13 is well documented for vesuvianites (Groat *et al.*, 1994*a*,*b*), Mn^{2+} was calculated as $Mn^{2+} = 2 - (Fe^{2+} + Mg^{2+} + Cu^{2+})$

dark-red internal reflections, smaller crystals are red to lilac and transparent. The crystals are characterized by prism faces: dominant [100], minor [110], both often with striations, terminated by [101].

At the N'Chwaning II mine, manganvesuvianite is also rock-forming, densely intergrown with either manganese-poor grossular or xonotlite and calcite in lenticular calcsilicate bodies within manganese ore beds. Those manganvesuvianite crystals are short to long prismatic (<0.2 mm) and strongly zoned. Additional associated minerals are calcite, serandite-pectolite, strontiopiemontite-tweddillite, mozartite and hydrogrossular-

TABLE 2. Single-crystal X-ray data collection and refinement of manganvesuvianite NCII-2.

Space group	*P4/n*, No. 85 (origin at $\bar{1}$)
a, *c* (Å), *V* (Å^3)	15.575(2), 11.824(2), 2868.5(6)
Crystal size (mm^3)	0.150 × 0.150 × 0.280
X-radiation	Mo-*K*α
Upper θ limit	30°
h, k, l limit	$21 \geqslant h \geqslant 0$, $21 \geqslant k \geqslant 0$, $16 \geqslant l \geqslant 0$
Reflections measured	4660
Unique reflections	4189
Reflections > 4σ (F)	3870
Absorption corr.	empirical: ψ scans
R_{int}, R_σ (%)	2.2, 1.4
Twinning, ratio	merohedral (110), 0.722(3): 0.278
Number of parameters	272; U_{eq} of Si sites constraint
*R*1 (on F) %	3.5
*wR*2 (on F^2) %	8.2

$$R1 = (\Sigma||F_0| - |F_c||)/(\Sigma|F_0|)$$

$$wR2 = \sqrt{\left(\sum\left(w(F_0^2 - F_c^2)^2\right)\right)/\left(\sum w(F_0^2)^2\right)}$$

henritermierite. Manganvesuvianite from the N'Chwaning II mine has been deposited (NMBE 35474) at the Natural History Museum in Bern, Switzerland.

Physical and optical properties

The megascopic colour is deep maroon-red with vitreous lustre. Other properties: the streak is colourless; Mohs' hardness: 6–7; brittle tenacity; cleavage not observed; and subchoncoidal fracture. The density was not measured because of strong chemical zoning. The calculated density for crystal NCII-1 is 3.404 g/cm^3 using a cell volume of 2868.5 Å^3. The mineral is uniaxial negative. At 589 nm, crystal NCII-1 has the refractive indices ε = 1.731(1) and ω = 1.719(1); extrapolated from small prism measurements at 546 nm: ω = 1.7353, ε = 1.7236; at 576.9 nm: ω = 1.7320, ε = 1.7200; at 643.8 nm: ω = 1.7274, ε = 1.7159. The crystal is strongly pleochroic, E: yellowish, O: dark red. Some of the manganvesuvianites analysed by Armbruster and Gnos (2000*b*), in addition to Mn^{3+}, also exhibit significant Cu^{2+} leading to lilac hues parallel to O. Such crystals are often colour zoned (Fig. 1) where the dark red core is more Mn^{3+} rich (typically 6–9 wt.% MnO) and the lilac rim is less Mn^{3+}-rich (typically 1.5–5 wt.% MnO). Because of the strong chemical zoning, an X-ray powder pattern was not collected. In addition, manganvesuvianite cannot be distinguished from other vesuvianites (e.g. with Fe^{3+}, Cu^{2+} or Al on the square pyramidal *Y′* site) on the basis of its X-ray powder pattern.

Chemical composition

Vesuvianites were analysed with a Cameca SX-50 microprobe using beam conditions of 15 kV and 20 nA, wavelength-dispersive spectrometers, and when possible, an enlarged spot size of ~10 μm. Natural and synthetic minerals were used as standards. Results are given in Table 1. Even within one crystal the Mn^{3+} concentration is strongly variable. Mn^{3+} completely occupies the *Y′* site with square pyramidal coordination and may partly substitute the octahedral *Y* sites, commonly occupied by Al.

Crystal structure refinement

Single-crystal X-ray data collection on a maroon red crystal NCII-2 (for average chemical composition see Table 1) was performed with an ENRAF NONIUS CAD4 single crystal diffractometer with graphite monochromated Mo-*K*α X-radiation. Cell dimensions were refined from the angular settings of 20 reflections (16 0 0, 0 16 0, 0 0 16, 12 12 0, 12 12 8, and their symmetry equivalent reflections). Experimental details of the data collection and refinement are summarized

TABLE 3. Atomic positional parameters and B_{eq} values for manganvesuvianite NCII-2.

Atom	Population	*x/a*	*y/b*	*z/c*	B_{eq} (Å^2)
*Z*1*A*	Si	−1/4	1/4	0	0.734(7)*
*Z*1*B*	Si	−1/4	1/4	1/2	0.734(7)*
*Z*2*A*	Si	−0.04035(8)	0.31890(8)	0.1292(1)	0.734(7)*
*Z*2*B*	Si	−0.04115(8)	0.18017(8)	0.3719(1)	0.734(7)*
*Z*3*A*	Si	0.08686(7)	0.34911(7)	−0.1352(1)	0.734(7)*
*Z*3*B*	Si	0.08199(7)	0.15100(7)	0.6357(1)	0.734(7)*
*Y*2*A*	0.90(1)Al + 0.10Mn	0	0	0	0.69(3)
*Y*2*B*	0.95(1)Al + 0.05Mn	−1/2	0	1/2	0.69(4)
*Y*3*A*	0.81(1)Al + 0.19Mn	−0.11226(7)	0.11962(7)	0.12497(9)	0.73(2)
*Y*3*B*	0.84(1)Al + 0.16Mn	−0.38839(7)	0.12156(7)	0.37384(9)	0.74(2)
*X*1	Ca	−1/4	1/4	0.2504(1)	0.81(1)
*X*2*A*	Ca	0.18951(6)	−0.04395(6)	0.62112(7)	0.84(1)
*X*2*B*	Ca	−0.04570(6)	0.18816(5)	−0.12041(7)	0.81(1)
*X*3*A*	Ca	0.09891(6)	0.17897(6)	0.11669(8)	1.35(1)
*X*3*B*	Ca	−0.39895(6)	−0.18214(6)	−0.39052(8)	1.27(1)
O1*A*		−0.2212(2)	0.1725(2)	0.0858(2)	0.86(4)
O1*B*		−0.2808(2)	0.1724(2)	0.4148(2)	0.84(4)
O2*A*		−0.1174(2)	0.3385(2)	0.2212(3)	0.98(4)
O2*B*		−0.1177(2)	0.1588(2)	0.2803(3)	0.90(4)
O3*A*		−0.0470(2)	0.2219(2)	0.0751(3)	0.94(4)
O3*B*		−0.0478(2)	0.2767(2)	0.4253(3)	0.80(4)
O4*A*		−0.0614(2)	0.3934(2)	0.0321(3)	1.01(5)
O4*B*		−0.0620(2)	0.1059(2)	0.4711(2)	0.88(4)
O5*A*		−0.0104(2)	0.3272(2)	−0.1771(3)	1.16(5)
O5*B*		−0.0150(2)	0.1701(2)	0.6797(3)	1.08(5)
O6*A*		0.1256(2)	0.2728(2)	−0.0572(3)	1.37(5)
O6*B*		0.1181(2)	0.2285(2)	0.5598(3)	1.34(5)
O7*A*		0.0561(2)	0.3262(2)	0.1805(3)	1.24(5)
O7*B*		0.0554(2)	0.1722(2)	0.3232(3)	1.06(5)
O8*A*		0.0928(2)	0.4386(2)	−0.0660(3)	0.84(4)
O8*B*		0.0909(2)	0.0610(2)	0.5678(3)	0.95(5)
O9		0.1479(2)	0.3562(2)	−0.2496(3)	1.09(5)
O10*A*		1/4	1/4	0.1344(5)	1.34(7)
O10*B*		−1/4	−1/4	−0.3648(5)	1.27(8)
O11*A*	OH	−0.0048(2)	0.0600(2)	0.1367(3)	0.95(5)
O11*B*	OH	−0.4960(2)	0.0626(2)	0.3645(3)	1.02(5)
X′4*B*	0.324(8) Ca	1/4	1/4	−0.1469(5)	1.1(1)
Y′1*B*	0.324(8) Mn	1/4	1/4	0.5428(3)	0.92(9)
X′4*A*	0.676(8) Ca	1/4	1/4	0.6475(2)	0.95(3)
Y′1*A*	0.676(8) Mn	1/4	1/4	−0.0454(2)	0.81(3)

Refined formula $Ca_{19}Mn_{2.72}Al_{10.28}Si_{18}O_{69}(OH)_9$; notice that due to similarity in X-ray scattering behaviour the pairs Fe,Mn and Al,Mg can not be distinguished.

To reduce the number of parameters, the Si displacement parameters were refined isotropically and constrained to identical values.

Note that in this paper we used the site nomenclature scheme of Groat (1992*b*) which is different from the scheme used by us in previous papers on vesuvianite (Armbruster and Gnos, 2000*a,b,c*).

in Table 2. Data reduction, including background and Lorentz polarization correction was carried out with the SDP program system (Enraf Nonius, 1983). The crystal did not show systematic extinctions of X-ray reflections. This is characteristic of low-*T* vesuvianites assembled of *P*4/*n* and *P*4*nc* polymorphs (e.g. Allen and Burnham, 1992; Armbruster and Gnos, 2000*a,b,c*). However,

TABLE 4. Selected interatomic distances of manganvesuvianite.

*Z*1*A*– O1*A* 4x	1.639(3)	*X*1– O1*A* 2×	2.333(3)
		O1*B* 2×	2.339(3)
*Z*1*B*– O1*B* 4x	1.646(3)	O2*A* 2×	2.507(3)
		O2*B* 2×	2.528(3)
*Z*2*A*– O7*A*	1.625(3)	mean	2.427
O3*A*	1.644(3)		
O2*A*	1.648(3)	*X*2*A*– O8*B*	2.329(3)
O4*A*	1.665(3)	O5*B*	2.337(3)
mean	1.646	O3*B*	2.375(3)
		O2*B*	2.410(3)
*Z*2*B*– O7*B*	1.615(3)	O5*A*	2.456(3)
O3*B*	1.635(3)	O4*B*	2.463(3)
O2*B*	1.645(3)	O1*B*	2.491(3)
O4*B*	1.679(3)	O6*B*	2.920(3)
mean	1.644	mean	2.473
*Z*3*A*– O8*A*	1.620(3)	*X*2*B*– O8*A*	2.329(3)
O6*A*	1.621(3)	O5*A*	2.333(3)
O5*A*	1.630(4)	O3*A*	2.371(3)
O9	1.657(4)	O4*A*	2.426(3)
mean	1.632	O2*A*	2.427(3)
		O5*B*	2.428(3)
*Z*3*B*– O6*B*	1.606(3)	O1*A*	2.462(3)
O8*B*	1.622(3)	O6*A*	3.068(3)
O5*B*	1.625(3)	mean	2.481
O9	1.664(4)		
mean	1.629	*X*3*A*– O7*A*	2.364(3)
		O3*A*	2.420(3)
*Y*2*A*– O11*A* 2×	1.869(3)	O11*A*	2.469(3)
O8*A* 2×	1.901(3)	O7*A*	2.505(4)
O4*A* 2×	1.953(3)	O7*B*	2.536(3)
mean	1.908	O6*A*	2.556(3)
		O10*A*	2.609(1)
*Y*2*B*– O11*B* 2×	1.876(3)	O8*A*	2.609(3)
O8*B* 2×	1.884(3)	mean	2.509
O4*B* 2×	1.941(3)		
mean	1.900	*X*3*B*– O7*B*	2.340(3)
		O3*B*	2.441(3)
*Y*3*A*– O11*A*	1.919(3)	O6*B*	2.452(3)
O2*B*	1.937(3)	O11*B*	2.498(3)
O1*A*	1.943(3)	O7*B*	2.508(3)
O3*A*	1.980(3)	O10*B*	2.567(1)
O5*A*	2.041(4)	O7*A*	2.583(4)
O4*A*	2.069(3)	O8*B*	2.608(3)
mean	1.982	mean	2.500
*Y*3*B*– O2*A*	1.911(3)	*X*4′*A*– O6*B* 4x	2.325(4)
O11*B*	1.915(3)	O9 4x	2.597(3)
O1*B*	1.915(3)	mean	2.461
O3*B*	1.967(3)		
O5*B*	1.997(4)	*X*4′*B*– O6*A* 4x	2.237(4)
O4*B*	2.057(3)	O9 4x	2.596(4)
mean	1.960	mean	2.417
Y′1*A*–O6*A* 4x	1.975(4)		
O10*A*	2.125(7)		
Y′1*B*– O6*B* 4x	2.091(4)		
O10*B*	2.105(8)		

reflections of the type *hk*0 with $h + k = 2n + 1$ were mostly weak and were ignored. The strongest reflections of this type were 1 6 0, 1 10 0, 2 7 0, and 2 15 0 with $10 < I/\sigma(I) < 15$. Reflections of the type 0*kl* with $k + l = 2n + 1$ and of the type *hhl* with $l = 2n + 1$ were considerably stronger indicating predominance of the *P*4/*n* polytype. Subsequently, the structure refinement was carried out in space group *P*4/*n* using the program SHELX-97 (Sheldrick, 1997) and applying the *P*4/*n* starting coordinates given by Armbruster and Gnos (2000*a*). Note that in this paper we use the site nomenclature scheme of Groat *et al.* (1992*b*) which is different from the scheme used by us in previous papers on vesuvianite (Armbruster and Gnos, 2000*a,b,c*).

Crystal structure of manganvesuvianite

The structurally investigated crystal (NCII-2) represents an intergrowth of polymorphs with *P*4/*n* and *P*4*nc* symmetry. A distinction of the two polymorphs is possible on the basis of characteristic X-ray reflections (e.g. Armbruster and Gnos, 2000*a,b,c*). However, the *P*4/*n* polymorph is more dominant and so a structure refinement in space group *P*4/*n* was successful. The crystal exhibits merohedral [110] twinning that converged to a refined twin ratio of 0.722(3)/0.278. In addition to twinning, there is occupational disorder leading to string A and B occupations (e.g. Armbruster and Gnos, 2000*a,b,c*) of 67.2(8) and 32.8%, respectively. This disorder could be an artifact caused by the presence of the subordinate *P*4*nc* polymorph.

*Z*1*A,B* and *Z*2*A,B* are orthosilicate groups whereas *Z*3*A* and *Z*3*B* form a disilicate unit with an angle *Z*3*A*–O9–*Z*3*B* of 136.1(2)°. The strong bending of the angle is balanced by increased *Z*3—O9 distances to increase Si—Si separation. In a previous study on Mn-bearing vesuvianites, which now have also to be considered manganvesuviantes, Armbruster and Gnos (2000*b*) noticed tetrahedral vacancies on the orthosilicate groups associated with increased Si—O distances. This unusual behaviour was interpreted as an indication of a hydrogarnet-like substitution in vesuvianite. Evidence of a hydrogarnet-like substitution in vesuvianite has also been reported by Henmi *et al.* (1994). The present structure refinement of manganvesuvianite did not show this hydrogarnet-like substitution. Average Si1—O and Si2—O distances (1.639—1.646 Å) are in the same range as found for many vesuvianites in

the literature (see Fig. 6 of Groat *et al.*, 1992*a*) and tetrahedral vacancies could also not be identified. The *Y*3*A,B* octahedra accept about twice as much Mn as the *Y*2*A,B* octahedra (Table 3). In addition, mean *Y*3*A,B*—O distances are slightly longer than *Y*2*A,B*—O distances (Table 4). The mean *Y*3*A*—O distance is significantly longer than the corresponding *Y*3*B*—O distance. As shown by neutron diffraction of a *P*4/*n* vesuvianite of the approximate composition $Ca_{19}Mg_2Al_{10}Fe^{3+}Si_{18}O_{69}(OH)_9$ (Pavese *et al.*, 1998) the *Y*3 sites are also the preferred positions for octahedral Mg^{2+}. Because Al and Mg have very similar scattering power for X-rays these elements cannot by distinguished in routine structure refinements. The larger size of *Y*3*A* compared to *Y*3*B* (Table 4) may be interpreted by incorporation of divalent cations (mainly Mg with minor Mn^{2+}) on *Y*3*A*. The *Y*′1*A* and *Y*′1*B* sites are partially occupied (67.2(8) and 32.8%, respectively) by Mn^{3+} leading to a characteristic Jahn-Teller distortion for the *Y*′1*A* site with Mn^{3+}—O distances of 1.975(4) Å forming the base and 2.125(7) Å forming the height of the square pyramid.

Tweddillite

General aspects of epidote-group crystal chemistry

The crystal structure of monoclinic epidote-group minerals (space group $P2_1/m$) comprises di-(Si_2O_7) and ortho-silicate (SiO_4) units linked to two kinds of chains (parallel to the *b* axis) built by edge-sharing octahedra. One chain consists of *M*2 octahedra while the other chain comprises *M*1 octahedra with *M*3 octahedra attached on alternate sides along its length. An OH-group is bonded to *M*2 octahedra. This arrangement gives rise to two types of cavities, a smaller one named *A*1, occupied by Ca and Mn^{2+} (nine-coordinated by oxygen), and a larger one named *A*2, occupied by Ca, Sr, Pb and *REE* (ten-coordinated by oxygen). Table 5 lists the chemical characteristics of all minerals in this group. If we exclude the REE^{3+} members of the epidote-group, substitution of octahedral Al by Fe^{3+}, Mn^{3+}, V^{3+} occurs preferentially on *M*3. An exception is the new mineral tweddillite with (Mn^{3+}, Fe^{3+}) on *M*3 and *M*1.

Name and defintion

The name is in honour of the first curator of the Museum of the Geological Survey at Pretoria, Republic of South Africa, Samuel Milbourn Tweddill FGS, who ran the Museum from 1897 to 1916.

Tweddillite is an epidote-group mineral; closely related to strontiopiemontite, but normalized to 8 cations, tweddillite has $Mn^{3+} + Fe^{3+} > 1.5$ p.f.u. and $Mn^{3+} > Fe^{3+}$. Tweddillite is the first epidote-group mineral that has in its end-member composition 2 ($Mn^{3+} + Fe^{3+}$) p.f.u. ($Mn^{3+} + Fe^{3+}$) occupy the *M*1 and *M*3 sites whereas *M*2 is occupied by Al. The simplified formula is $CaSr(Mn^{3+},Fe^{3+})_2Al\{Si_3O_{12}\}(OH)$.

TABLE 5. Cation distribution and O4 occupancy in monoclinic epidote-group minerals (space group $P2_1/m$).

Name	*A*1	*A*2	*M*1	*M*2	*M*3	O4
Clinozoiste	Ca	Ca	Al	Al	Al	O
Epidote	Ca	Ca	Al	Al	Fe^{3+}	O
Mukhinite	Ca	Ca	Al	Al	V^{3+}	O
Hancockite	Ca	Pb	Al	Al	Fe^{3+}	O
Piemontite	Ca	Ca	Al	Al	Mn^{3+}	O
Strontiopiemontite	Ca	Sr	Al	Al	Mn^{3+}	O
Tweddillite	Ca	Sr	Mn^{3+}	Al	Mn^{3+}	O
REE-bearing minerals of the epidote-group						
Dissakisite	Ca	REE^{3+}	Al	Al	Mg	O
Allanite	Ca	REE^{3+}	Al	Al	Fe^{2+}	O
Androsite	Mn^{2+},Ca	REE^{3+}	Mn^{3+}	Al	Mn^{2+}	O
Khristovite	Ca	REE^{3+}	Mg	Al	Mn^{2+}	F
Dollaseite	Ca	REE^{3+}	Mg	Al	Mg	F

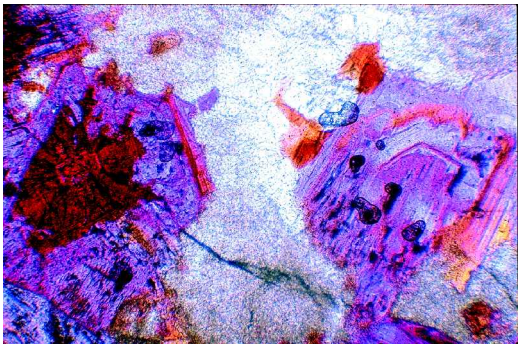

FIG. 1. Thin-section of strongly zoned manganvesuvianite in a grossular matrix (sample NC14). The dark red vesuvianite cores typically contain 6–9 wt.% MnO, lilac zones contain 1.5–5 wt.% MnO. Base of photograph is 1 mm long; plane polarized light.

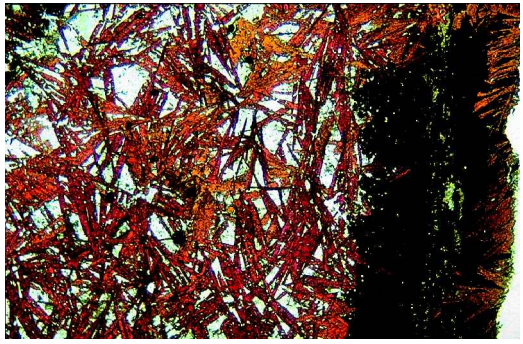

FIG. 2. Thin-section of tweddillite blades (red-orange) in a matrix of serandite-pectolite (white). The opaque mineral is braunite. Base of photograph is 3.2 mm long; plane polarized light.

Identification criteria

(1) Tweddillite is optically very similar to strontiopiemontite (Bonazzi *et al.*, 1990; Catti *et al.*, 1989) but has a higher average refractive index (n = 1.825 *vs.* n = 1.763 for strontiopiemontite) because of its higher Mn content.

(2) Chemical analyses (normalized to 8 cations) yield $Mn^{3+} + Fe^{3+} > 1.5$ and $Mn^{3+} > Fe^{3+}$. Note that several piemontites and strontiopiemontites have Sr + Ca < 2 a.p.f.u. Thus, additional Mn^{2+} has been assumed to substitute for Sr + Ca. To properly evaluate the Mn^{3+} concentration, Mn^{2+} must be calculated as Mn^{2+} p.f.u. = 2 − (Sr + Ca) p.f.u.

(3) Crystal structure analysis of tweddillite indicates that trivalent transition metals (Mn^{3+} + Fe^{3+}) occupy the octahedral *M*3 position and dominate the octahedral *M*1 site.

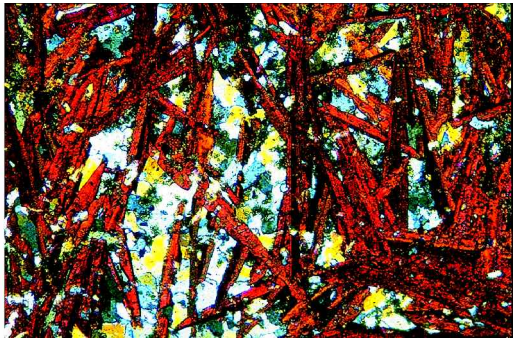

FIG. 3. Thin-section of (100) twinned tweddillite blades (red-orange-magenta) in a matrix of serandite-pectolite (white-grey-yellow). Base of photograph is 1 mm long; crossed polars.

TABLE 6. Observed and calculated X-ray powder pattern for tweddillite.

h	*k*	*l*	$d_{obs.}$	$d_{calc.}$	$I/I_{obs.}$	$I_{calc.}$
1	0	−1	7.99	8.00	10	30
1	0	−2*	5.17	5.08	10	30
1	1	0	4.675	4.665	10	10
2	0	−2	4.000	4.002	10	13
2	1	−1	3.513	3.515	50	50
1	1	−3	2.936	2.942	100	100
3	0	−2	2.936	2.931	overlap	20
0	2	0	2.854	2.849	40	30
0	1	3	2.739	2.741	10	30
3	0	0	2.703	2.708	80	20
2	0	2	2.586	2.584	80	30
1	2	−2	2.482	2.484	10	10
3	1	−3	2.415	2.416	30	17
2	2	−2	2.320	2.321	30	10
4	0	−1	2.182	2.185	80	20
2	2	1	2.149	2.147	40	20
2	2	−3	2.126	2.129	30	10
3	1	2	1.8957	1.8963	30	5
2	2	−4	1.8957	1.8950	overlap	20
4	1	−5	1.7178	1.7168	30	6
1	0	−6	1.6695	1.6688	30	10

Refined cell dimension based on 20 indexed reflections (the starred reflection was not used for refinement): a = 8.932(5), b = 5.698(4), c = 10.310(5) Å, β = 114.56(4), V = 477.3(8) Å^3

Occurrence

Tweddillite occurs in calcsilicate rocks formed as hydrothermal alteration of primary sedimentary manganese ore in the Wessels mine of the Kalahari manganese field (South Africa). The crystals form dark-red 'suns' of very thin (~0.02 mm) radiating (001) blades, elongated parallel to {010} (up to 0.5 mm), on the hanging wall of the ore-body. All crystals are (100) twinned. Associated minerals are serandite-pectolite and braunite. A sample of tweddillite has been deposited (NMBE 35475) at the Natural History Museum, Bern, Switzerland.

Recently, Enami and Banno (2001) presented analyses of strontiopiemontites which also fulfill the definition of tweddillite. However, the Sr concentration is considerably <1 p.f.u. but instead Ba and Pb complete the *A*2 occupancy. These tweddillites were found together with braunite and hollandite minerals in a piemontite quartzose

TABLE 7. Electron microprobe analyses of tweddillite.

Oxide	Twe-core[1]	Range	Twe-rim[1]	Range	Min. Al[2]	Twe-2[3]	Range
SiO_2	32.74	32.61–32.90	32.47	32.22–32.60	32.50	32.58	31.67–33.05
Al_2O_3	13.29	12.74–13.55	11.66	11.42–12.11	9.35	11.85	9.35–13.47
Fe_2O_3	4.04	3.56–4.42	2.74	1.92–4.27	5.80	3.41	2.40–5.80
Mn_2O_3	19.56	19.26–19.97	22.34	20.90–23.44	21.32	20.97	19.73–22.29
MgO					0.00	0.04	0.00–0.06
CuO					0.00	0.02	0.00–0.08
CaO	10.52	10.01–11.29	10.47	10.01–10.85	9.78	10.25	9.78–10.87
SrO	17.11	16.14–18.76	16.86	15.62–18.43	18.18	16.94	16.24–18.18
BaO					0.10	0.46	0.10–0.81
PbO					1.42	2.08	0.50–4.76
Na_2O	0.03	0.00–0.04	0.01	0.00–0.05	0.01	0.03	0.00–0.06
K_2O					0.01	0.00	0.00–0.03
F					0.00	0.01	0.00–0.09
Cl					0.01	0.01	0.00–0.05
H_2O (calc.)	1.44		1.41		1.48	1.50	1.47–1.54
–(F+Cl)					0.00	–0.01	–0.04–0.00
Sum	97.13	96.43–98.45	96.27	95.87–97.59	99.96	100.14	98.79–101.23
Formulae normalized to 8 cations							
Si	2.992		3.011		3.038	3.005	
Al	1.431		1.274		1.030	1.288	
Fe^{3+}	0.278		0.191		0.408	0.237	
Mn^{3+}	1.360		1.577		1.517	1.472	
Mg					0.000	0.005	
Cu					0.000	0.001	
Ca	1.030		1.040		0.979	1.012	
Sr	0.904		0.904		0.985	0.906	
Ba					0.004	0.017	
Pb					0.036	0.052	
Na	0.005		0.002		0.001	0.006	
K					0.001	0.000	
F					0.001	0.004	
Cl					0.002	0.001	
OH					0.997	0.995	
Σ $Me^{2+,1+}$	1.939		1.946		2.006	1.999	
Σ Me^{3+}	3.069		3.042		2.955	2.996	

[1] Average of four analyses
[2] Analysis with lowest Al concentration
[3] Average of 17 analyses

TABLE 8. Single-crystal X-ray data collection and refinement of tweddillite.

Space group	$P2_1/m$, No. 11
a, b, c (Å), β(°)	8.934(5), 5.718(2), 10.325(5), 114.54(1)
V (Å^3)	479.8
Crystal size (mm^3)	0.01 × 0.140 × 0.260
X-radiation	Mo*K*-α
Upper θ limit	28°
h, k, l limit	$11 \geqslant h \geqslant -11$, $7 \geqslant k \geqslant -7$, $13 \geqslant l \geqslant -13$
Reflections measured	3315
Reflections > 4σ (F)	2499
Absorption corr.	Empirical: ψ scans
R_σ (%)	4.2
Twinning, ratio	on (100), 0.459(2): 0.541
Number of parameters	122; U_{iso} of H fixed at 0.05 Å^2
*R*1 (on F) %	5.9
*wR*2 (on F^2) %	17.6

$$R1 = (\Sigma||F_0| - |F_c||)/(\Sigma|F_0|)$$

$$wR2 = \sqrt{\left(\sum\left(w(F_0^2 - F_c^2)^2\right)/\left(\sum w(F_0^2)^2\right)\right)}$$

schist of the Sanbagawa metamorphic belt, central Shikoku, Japan. For these samples *P-T* conditions at 480–580°C and 0.7 1.0 GPa have been estimated.

Physical and optical properties

The megascopic colour is deep dark-red with vitreous lustre. Additional properties are: the streak is brownish-red, Mohs' hardness: 6–7, brittle tenacity, perfect cleavage on (001), subchoncoidal fracture. The density was not measured because of strong chemical zoning and intimate intergrowth with serandite-pectolite. The calculated density is 3.816 g/cm^3 (core) to 3.873 g/cm^3 (rim), both calculated with cell volume of 477.8 Å^3. The mineral is biaxial positive, only an average refractive index was determined by immersion methods: n = 1.825. Due to the thin nature of the blades the exact optical orientation could not be determined. Tweddillite is strongly pleochroic (Figs 2 and 3). Within the (001) blades, the crystals appear dark red parallel to *b* and orange-yellow parallel to *a*. Perpendicular to (001) the blades appear magenta to red.

X-ray powder pattern

An X-ray powder pattern was recorded with a diffractometer using Cu-$K\alpha_1$ X-radiation (Table 6). Intensities were estimated from peak heights and are strongly influenced by admixed serandite-pectolite and braunite. $I_{calc.}$ was determined from the refined structural parameters obtained from single-crystal X-ray data. The cell dimensions from powder data converged at a = 8.932(5), b = 5.698(4), c = 10.310(5) Å, β = 114.56(4), V = 477.3(8) Å^3.

Chemical composition

Tweddillite (Table 7) was analysed with a Cameca SX-50 microprobe using beam conditions of 15 kV and 20 nA, wavelength-dispersive spectrometers, and an enlarged spot size of ~10 µm. Natural and synthetic minerals were used as standards. H_2O/OH could not be analysed by a proton-sensitive method because of intimate intergrowth between tweddillite and pectolite (OH-bearing). The first set of analyses (Table 7, Twe-core and Twe-rim) displayed rather low oxide sums, so in a second set of analyses, of a different section but produced from the same hand specimen, additional elements (e.g. Pb and Ba) were analysed. Addition of these elements increased the oxide sums to the expected range.

Crystal structure refinement

All tested tweddillite crystals were twinned parallel to (100). In the reciprocal lattice, two

a^*c^* layers are superimposed with a common a^*. For one twin individual the angle between a^* and c^* is 114.5° and for the other twin individual the angle is 180−114.5°. Layers from the two twin individuals with l = 0, 4, 7 and 11 coincide. Layers with l = 2, 5, 9 and 13 can be resolved for the two individuals and the other layers partly overlap. The same type of twinning has been described for strontiopiemontite (Bonazzi *et al.*, 1990). Twin X-ray data collection (Table 8) was performed with a CCD-detector-equipped Siemens SMART three-circle diffractometer using graphite monochromated Mo-$K\alpha$ radiation. The TWIN software utility allowed the orientation matrices of both twin individuals to be determined and the cell dimensions to be refined. Using the HKLF 5 option a reflection file was created containing indices and intensity data for both individuals. This reflection file was processed by the program SHELX-97 (Sheldrick, 1997). The coordinates for strontiopiemontite by Bonazzi *et al.* (1990) were used as starting positions. Initially, the populations of all *M* and *A* sites were refined alternately. It was found that *A*1 and *A*2 are occupied by Ca and Sr, respectively, and these occupations were subsequently fixed. *M*2 and *M*3 revealed pure Al and Mn occupation, and these values were also fixed. Thus, only the Al-Mn concentration on *M*1 was allowed to vary in the final refinement (Table 9). The hydrogen position (H10) was extracted from the difference Fourier map and was restrained to be 0.90(5) Å apart from O10, forming the OH group. All atoms except H were refined with anisotropic displacement parameters. Additional details are given in Table 8.

Crystal structure of tweddillite

Structure refinements on strontiopiemontite were published by Bonazzi *et al.* (1990). However, in these crystals the *A*2 site was only occupied by 0.59 and 0.73 Sr, respectively, with the remainder being Ca. A synthetic piemontite (MK42/1) of $Ca_2Mn^{3+}_{1.391}Al_{1.609}Si_3O_{12}(OH)$ composition produced at 800°C and 15 kbar (Mn_2O_3−MnO_2 buffer) by Kersten *et al.* (1987) was refined by Almen (1987). Site population refinements of the tweddillite studied by X-ray diffraction (Table 9) converged at the composition $CaSr(Mn^{3+},Fe^{3+})_{1.58}Al_{1.42}Si_3O_{12}(OH)$, close to the crystal core composition given in Table 7. In

TABLE 9. Atomic positional parameters and B_{eq} values for tweddillite.

Atom	Population	*x/a*	*y/b*	*z/c*	B_{eq} (Å^2)
*A*1	1 Ca	0.7646(2)	3/4	0.1575(2)	0.92(3)
*A*2	1 Sr	0.5941(1)	3/4	0.42163(8)	1.03(1)
Si1		0.3417(3)	3/4	0.0411(3)	0.95(4)
Si2		0.6877(3)	1/4	0.2787(3)	0.85(4)
Si3		0.1803(3)	3/4	0.3150(2)	0.86(4)
*M*1	0.57(1)Mn+0.43Al	0	0	0	0.64(3)
*M*2	1 Al	0	0	1/2	0.66(4)
*M*3	1 Mn	0.2954(2)	1/4	0.2181(1)	0.90(2)
O1		0.2389(5)	0.9915(7)	0.0386(4)	1.42(9)
O2		0.2984(5)	0.9786(6)	0.3480(4)	1.14(8)
O3		0.7967(5)	0.0160(6)	0.3433(4)	1.17(7)
O4		0.0600(7)	1/4	0.1312(6)	0.9(1)
O5		0.0369(7)	3/4	0.1479(6)	1.0(1)
O6		0.0661(7)	3/4	0.4061(6)	1.0(1)
O7		0.5174(8)	3/4	0.1691(6)	1.4(1)
O8		0.5277(6)	1/4	0.3110(6)	1.0(1)
O9		0.6323(7)	1/4	0.1063(6)	1.8(1)
O10		0.0815(7)	1/4	0.4293(6)	0.9(1)
H10		0.06(1)	1/4	0.339(6)	3.95

Refined formula: $CaSrMn_{1.58}Al_{1.42}Si_3O_{12}(OH)$. Note that due to similarity in X-ray scattering behaviour Fe and Mn cannot be distinguished.

TABLE 10. Selected interatomic distances in tweddillite and related compounds (SRPM: strontiopiemontite (Bonazzi *et al.*, 1990); MK42/1: Mn^{3+}-rich piemontite (Almen, 1987)).

		Tweddi	SRPM	MK42/1
*A*1–	O7	2.260(7)	2.227(13)	2.296(2)
	O3 (2×)	2.370(4)	2.324(9)	2.305(2)
	O1 (2×)	2.497(4)	2.455(8)	2.445(3)
	O5	2.475(6)	2.509(12)	2.542(2)
	O6	2.846(6)	2.857(9)	2.934(3)
	O9 (2×)	3.055(3)	3.029(5)	3.079(1)
	mean	2.603	2.578	2.603
*A*2–	O7	2.405(6)	2.374(12)	2.254(4)
	O10	2.657(6)	2.608(10)	2.489(3)
	O2 (2×)	2.663(4)	2.614(8)	2.534(3)
	O2 (2×)	2.757(4)	2.715(8)	2.669(2)
	O3 (2×)	2.731(4)	2.722(9)	2.832(2)
	O8 (2×)	3.044(2)	3.019(4)	3.037(1)
	mean	2.745	2.712	2.689
Si1–	O7	1.577(6)	1.573(10)	1.557(3)
	O9	1.633(6)	1.591(15)	1.638(4)
	O1 (2×)	1.653(4)	1.648(8)	1.646(2)
	mean	1.629	1.615	1.622
Si2–	O8	1.597(5)	1.608(15)	1.605(2)
	O3 (2×)	1.626(4)	1.618(8)	1.619(2)
	O9	1.637(6)	1.637(15)	1.646(4)
	mean	1.622	1.620	1.622
Si3–	O2 (2×)	1.624(4)	1.606(8)	1.625(2)
	O6	1.651(6)	1.638(15)	1.640(3)
	O5	1.668(6)	1.667(10)	1.656(4)
	mean	1.642	1.629	1.637
*M*1–	O4 (2×)	1.887(4)	1.866(7)	1.881(5)
	O1 (2×)	2.002(4)	1.947(7)	1.973(1)
	O5 (2×)	2.017(4)	1.975(8)	2.014(2)
	mean	1.969	1.929	1.956
*M*2–	O10 (2×)	1.867(4)	1.862(9)	1.889(2)
	O3 (2×)	1.883(4)	1.865(6)	1.856(2)
	O6 (2×)	1.951(4)	1.928(9)	1.944(2)
	mean	1.900	1.885	1.896
*M*3–	O8	1.890(5)	1.855(10)	1.851(3)
	O4	1.913(6)	1.911(11)	1.882(2)
	O2 (2×)	2.045(4)	2.031(8)	2.045(3)
	O1 (2×)	2.258(4)	2.270(8)	2.277(3)
	mean	2.068	2.061	2.063

Tweddi: $CaSr(Mn^{3+}, Fe^{3+})_{1.58}Al_{1.42}Si_3O_{12}(OH)$
SRPM: $Ca_{1.05}Mn_{0.22}Sr_{0.73}(\underline{Mn}^{3+},Fe^{3+})_{1.20}Al_{1.80}\ Si_3O_{12}(OH)$
MK42/1: $Ca_2Mn^{3+}{}_{1.391}Al_{1.609}Si_3O_{12}(OH)$

Table 10, selected bond distances of tweddillite are compared with strontiopiemontite, crystal SRPM (Bonazzi *et al.*, 1990) and synthetic piemontite, crystal MK42/1 (Almen, 1987).

Crystal SRPM has the shortest mean *A*1–O distance which can be explained by the mixed occupancy of *A*1 by 0.78 Ca and 0.22 Mn^{2+}. As expected tweddillite has the longest mean *A*2–O distance because this site is completely occupied by Sr whereas *A*2 in MK42/1 is a pure Ca site and *A*2 in SRPM has a mixed occupation of 0.73 Sr and 0.27 Ca. The mean size of the *M*1 site is governed by the (Mn^{3+} + Fe^{3+}) occupancy on this position. The structure refinements yielded the following (Mn^{3+} + Fe^{3+}) occupancies: 0.22 (SRPM), 0.46 (MK42/1) and 0.58 (tweddillite). In all three structures *M*2 is completely occupied by Al. The mean size of *M*3 is also very similar because of the similar (Mn^{3+} + Fe^{3+}) occupancy: 0.98 (SRPM), 0.93 (MK42/1), and 1.00 (tweddillite). Ferraris *et al.* (1989) conducted a neutron diffraction study of a strontian piemontite and resolved the Fe^{3+}/Mn^{3+} distribution on *M*1 and *M*3 yielding the composition $Ca(Ca_{0.84}Sr_{0.16})^{M1}(Al_{0.81}Mn_{0.17}Fe_{0.02})^{M2}(Al)^{M3}(Al_{0.06}Mn_{0.61}Fe_{0.33})\{Si_3O_{12}\}(OH)$. This indicates that, relative to Fe^{3+}, the *M*1 site is preferred by Mn^{3+} (Mn/Fe = 8.5 on *M*1 *vs.* Mn/Fe = 1.85 on *M*3).

Strontiopiemontite (SRPM) and tweddillite are distinct from the synthetic piemontite (MK42/1) in the behaviour of the Si1–O9–Si2 bridging angle (154.6° in SRPM, 156.6° in tweddillite, but 147.4° in synthetic piemontite). Enami and Banno (2001) noticed that in natural piemontites and strontiopiemontites the average size of the cation (Ca + Sr + Ba + Pb) occupying *A*2 is positively correlated with the ionic radius of the octahedral *M* sites. In the Sr-free synthetic piemontite this balancing effect cannot operate and instead the Si1–O9–Si2 angle compresses. Similarly compressed angles of this type are known for allanites (Bonazzi and Menchetti, 1995).

References

Allen, F.M. and Burnham, C.W. (1992) A comprehensive structure-model for vesuvianite: Symmetry variations and crystal growth. *Canadian Mineralogist*, **30**, 1–18.

Almen, H. (1987) *Kristallchemie von Piemontiten, Änderung der Klinozoisitstruktur durch Einbau von dreiwertigem Mangan.* Diplomarbeit, Institut für Mineralogie und Kristallstrukturlehre, Universität Würzburg, Germany.

Armbruster, T. and Gnos, E. (2000*a*) *P*4/*n* and *P*4*nc* long-range ordering in low-temperature vesuvianites. *American Mineralogist*, **85**, 563–569.

Armbruster, T. and Gnos, E. (2000*b*) Tetrahedral vacancies and cation ordering in low-temperature Mn-bearing vesuvianites: Indication of a hydrogarnet-like substitution. *American Mineralogist*, **85**, 570–577.

Armbruster, T. and Gnos, E. (2000*c*) 'Rod' polytypism in vesuvianite: crystal structure of a low-temperature *P*4*nc* vesuvianite with pronounced octahedral cation ordering. *Schweizerische Mineralogische und Petrographische Mitteilungen*, **80**, 109–116.

Bonazzi, P. and Menchetti, S. (1995) Monoclinic members of the epidote group: Effects of the Al ↔ Fe^{3+} ↔ Fe^{2+} substitution and of the entry of REE^{3+}. *Mineralogy and Petrology*, **53**, 133–153.

Bonazzi, P., Menchetti, S. and Palenzona, A. (1990) Strontiopiemontite, a new member of the epidote group, from Val Graveglia, Liguria, Italy. *European Journal of Mineralogy*, **2**, 519–523.

Cairncross, B., Beukes, N. and Gutzmer, J. (1997) *The Manganese Adventure; The South African Manganese Fields.* Associated Ore and Metal Cooperation Limited, Marshalltown, Johannesburg 2107, Republic of South Africa, 236 pp.

Catti, M., Ferraris, G. and Ivaldi, G. (1989) On the crystal chemistry of strontian piemontite with some remarks on the nomenclature of the epidote group. *Neues Jahrbuch für Mineralogie Monatshefte*, **1989**, 357–366.

Enami, M. and Banno, Y. (2001) Partitioning of Sr between coexisting minerals of the hollandite- and piemontite-groups in quartz-rich schist from the Sanbagawa metamorphic belt, Japan. *American Mineralogist*, **86**, 205–214.

Enraf Nonius (1983) *Structure Determination Package (SDP).* Enraf-Nonius, Delft, The Netherlands.

Ferraris, G., Ivaldi, G., Fuess, H. and Gregson, D. (1989) Manganese/iron distribution in a strontian piemontite by neutron diffraction. *Zeitschrift für Kristallographie*, **187**, 145–151.

Fitzgerald, S., Rheingold, A.L. and Leavens, P.B. (1986) Crystal structure of a non-*P*4/*nnc* vesuvianite from Asbestos, Quebec. *American Mineralogist*, **71**, 1483–1488.

Giuseppetti, G. and Mazzi, F. (1983) The crystal structure of a vesuvianite with *P*4/n symmetry. *Tschermaks Mineralogische und Petrograpghische Mitteilungen*, **31**, 277–288.

Groat, L.A., Hawthorne, F.C. and Ercit, T.S. (1992*a*) The chemistry of vesuvianite. *Canadian Mineralogist*, **30**, 19–48.

Groat, L.A., Hawthorne, F.C. and Ercit, T.S. (1992*b*) The role of fluorine in vesuvianite: A crystal-structure study. *Canadian Mineralogist*, **30**, 1065–1075.

Groat, L.A., Hawthorne, F.C. and Ercit, T.S. (1994*a*) Excess *Y*-group cations in the crystal structure of vesuvianite. *Canadian Mineralogist*, **32**, 497–504.

Groat, L.A., Hawthorne, F.C. and Ercit, T.S. (1994*b*) The incorporation of boron into the vesuvianite structure. *Canadian Mineralogist*, **32**, 505–523.

Groat, L.A., Hawthorne, F.C. Ercit, T.S. and Grice, J.D. (1998) Wiluite, $Ca_{19}(Al,Mg,Fe,Ti)_{13}(B,Al)_5Si_{18}O_{68}(O,OH)_{10}$, a new mineral species isostructural with vesuvianite, from the Sakha Republic, Russian Federation. *Canadian Mineralogist*, **36**, 1301–1304.

Hålenius, U. and Annersten, H. (1994) Five-coordinated trivalent manganese in vesuvianite: A spectroscopic study. *Abstracts, International Mineralogical Association, 16th General Meeting, Pisa, Italy*, pp. 162–163.

Henmi, C., Kusachi, I. and Henmi, K. (1994) Vesuvianite from Kushiro Prefecture, Japan. *Abstracts, International Mineralogical Association, 16th General Meeting, Pisa, Italy*, p. 172.

Kersten, M., Langer, K., Almen, H. and Tillmanns, E. (1987) Kristallchemie von Piemontiten: Strukturverfeinerung und polarisierte Einkristallspektren. *Zeitschrift für Kristallographie*, **178**, 120–121.

Nickel, E.H. and Grice, J.D. (1998) The IMA Commission on New Minerals and Mineral Names: Procedures and guidelines on mineral nomenclature, 1998. *Canadian Mineralogist*, **36**, 913–926.

Ohkawa, M., Yoshiasa, A. and Takeno, S. (1992) Crystal chemistry of vesuvianite: Site preferences of square-pyramidal coordinated sites. *American Mineralogist*, **77**, 945–953.

Ohkawa, M., Yoshiasa, A. and Takeno, S. (1994) Structural investigation of high- and low-symmetry vesuvianite. *Mineralogical Journal*, **17**, 1–20.

Olejniczak, Z. and Zabinski, W. (1996) ^{27}Al NMR spectroscopic study of white vesuvianite from Piz Lunghin, Switzerland. *Mineralogia Polonica*, **27**, 41–44.

Pavese, A., Prencipe, M., Tribaudino, M. and Aagaard, St.S. (1998) X-ray and neutron single-crystal study of *P4/n* vesuvianite. *Canadian Mineralogist*, **36**, 1029–1037.

Phillips, B.L., Allen, F.M. and Kirkpatrick, R.J. (1987) High-resolution solid-state ^{27}Al NMR spectroscopy of Mg-rich vesuvianite. *American Mineralogist*, **72**, 1190–1194.

Platonov, A.N., Zabinski, W. and Sachanbinski, M. (1995) Optical absorption spectra of Mn^{3+} ions in vesuvianites from Lower Silesia, Poland. *European Journal of Mineralogy*, **7**, 1345–1352.

Sheldrick, G.M. (1997) *SHELX-97, program for crystal structure determination*. University of Göttingen, Germany.

{*Manuscript received 5 July 2001: revised 29 October 2001*}